Microchimica Acta (2021) 188: 395
https://doi.org/10.1007/s00604-021-05000-y

ORIGINAL PAPER

A novel aptasensor based on DNA hydrogel for sensitive visual detection of ochratoxin A

Liling Hao[1] · XuTao Liu[2] · Sunjie Xu[3] · Faliang An[3] · Huajie Gu[4] · Fei Xu[1]

Received: 26 April 2021 / Accepted: 24 August 2021 / Published online: 28 October 2021

Abstract

A novel visual detection mode is proposed to improve the detection sensitivity for the determination of ochratoxin A (OTA). The mode is based on aptamer recognition and the signal amplification of rolling circle amplification (RCA) products self-assembled DNA hydrogel. Moreover, gold nanoparticles (AuNPs) were directly assembled inside the DNA hydrogel by adjusting the padlock probe sequences to achieve a stronger binding force between the DNA hydrogel and AuNPs; this avoids the need for modification of AuNPs with DNA sequences. In the presence of OTA, DNA hydrogel is formed. With higher concentrations of OTA, a larger amount of DNA hydrogel is formed. When AuNPs are added to the DNA hydrogel, AuNPs can be enclosed inside the DNA hydrogel. With more DNA hydrogel, there is less AuNPs in the supernatant. Thus, the absorbance of the supernatant is anti-correlated with the concentration of OTA. After optimization of the experimental conditions, the change in the absorbance of the supernatant was linearly correlated with the concentration of OTA, in the range 0.05 to 10 ng/mL; the limit of detection was 0.005 ng/mL. The good specificity of the developed biosensor was confirmed in the presence of other mycotoxins that are coexistent with or analogues of OTA. By comparing the developed method with the ELISA method, the accuracy and stability of this new method were also verified, with good performance obtained in real samples.

Keywords Self-assembled rolling circle amplification · DNA hydrogel · Ochratoxin A · Mycotoxin · Photometric detection

Introduction

Mycotoxin contamination is one of the most important safety risks to food, crops, and produce. Ochratoxin A (OTA) pollution, a type of mycotoxin, occurs widely in wine, nuts, beer, coffee, cereals, wheat, and so on [1]. OTA is derived from *Aspergillus and Penicillium* spp. [2] and has been shown to be nephrotoxic, immunotoxic, teratogenic, and carcinogenic [3]. Therefore, the Chinese government and other organizations, such as the European Union, have established maximum residue limits (MRL) of OTA [4]. To ensure that all products meet these limits, it is necessary to develop efficient, sensitive, and rapid OTA detection methods. Various methods to detect OTA in food have been developed, such as visual biosensors [5, 6], fluorescent biosensors [7, 8], high-performance liquid chromatography (HPLC) [9], and surface-enhanced Raman scattering (SERS) [10], among others. Of these, visual detection is considered to be one of the most promising fast detection methods for on-site detection due to the determination of targets by colour change only.

DNA hydrogel is used in visual detection due to its specific nest-like structure, its programmability, and its three-dimensional macroscopic properties [11–13]. The specific nest-like structure can support enzymes and nanoparticles to achieve corresponding DNA hydrogel-specific properties. The programmability of DNA hydrogel provides convenience for the fabrication of target-responsive biosensors. The three-dimensional macroscopic properties make DNA hydrogel more suitable for visual detection, especially with the use of

✉ Fei Xu
xufei8135@126.com

[1] School of Medical Instrument and Food Engineering, Shanghai Engineering Research Center for Food Rapid Detection, University of Shanghai for Science and Technology, Shanghai 200093, People's Republic of China

[2] Samueli School of Engineering, University of California Los Angeles, Los Angeles 90026, USA

[3] State Key Laboratory of Bioreactor Engineering, East China University of Science and Technology, Shanghai 200237, People's Republic of China

[4] School of Chemistry and Life Sciences, Suzhou University of Science and Technology, Suzhou 215009, People's Republic of China

colorimetric reagents such as gold nanomaterials, which are supported by the specific nest-like structure of the DNA hydrogel [14–17].

Most of the published DNA hydrogel-based visual biosensors to date were designed based on hydrogel collapse caused by target detection. In this detection mode, DNA hydrogel is first formed by complementary hybridization between DNA sequences. The duplex inside the DNA hydrogel melts in the presence of the target due to the stronger combination between the aptamer and the target, resulting in the collapse of the preformed DNA hydrogel. The collapse of the DNA hydrogel further causes the release of signal molecules inside the DNA hydrogel; the amount of released signal molecules is related to the concentration of the target [18, 19]. However, the formation of DNA hydrogel is based on a complicated design of DNA sequences, and the collapse of the hydrogel requires the presence of a large amount of the target, resulting in insufficient sensitivity of the DNA hydrogel-based visual detection method [20].

DNA hydrogels based on self-assembled rolling circle amplification (RCA) products can provide an alternative approach to target detection [21, 22]. In this mode, only the sequences of the padlock probe and primer need to be designed; this avoids the complicated design of DNA sequences. Meanwhile, the DNA hydrogel is formed in the presence of the target, providing the possibility of higher sensitivity compared with the above approach where the hydrogel collapses in the presence of the target. RCA is an enzyme-dependent isothermal DNA amplification method mediated by a padlock probe and primer; the products consist of hundreds of repeated DNA sequences that are complementary to the padlock probe sequence [23–26]. RCA products can form a DNA hydrogel through liquid crystallization [23]. To date, there have been several reports of gold nanoparticle (AuNP)-based RCA products self-assembled DNA hydrogel [27]. However, the AuNPs used in these assays had to be modified by DNA sequences to achieve immobilization of the AuNPs inside the DNA hydrogel. This is inconvenient for in-field detection as the modification of AuNPs also requires the design of DNA sequences to modify the AuNPs.

Herein, we propose a versatile and convenient strategy to immobilize AuNPs inside DNA hydrogel. For this strategy, a visual aptasensor for sensitive detection of OTA was fabricated. In this work, AuNPs were directly assembled inside DNA hydrogel by adjusting the padlock probe DNA sequences to form a stronger binding force between the RCA products and AuNPs. The competition between the complementary sequence and OTA for the aptamer is utilized, and the released complementary sequence is used as the RCA reaction trigger. Thus, the RCA reaction only commences in the presence of OTA, resulting in the formation of the DNA hydrogel. AuNPs without DNA sequence modification are then added into the DNA hydrogel to form the AuNP functional DNA hydrogel. When a fixed amount of AuNPs is added, the higher the concentration of OTA, the more DNA hydrogel generated, the less AuNPs in the solution, and the lower the absorbance of the supernatant. Therefore, the concentration of OTA can be measured by determining the absorbance of the supernatant.

Materials and methods

Materials and instruments

The DNA sequences (Table S1) were purchased from Shanghai Sangon Biological Science & Technology Company (Shanghai, China). Ligases used in RCA were provided by New England Biolabs, Inc. (Ipswich, MA). Mycotoxins used in this work were provided by Qingdao Pribolab Biological Engineering Co., Ltd. (Qingdao, China). Mercaptopolyethylene glycol monomethyl ether 5000 (SH-PEG) and DNA marker were bought from Sigma-Aldrich (Sigma-Aldrich LLC.). Chloroauric acid, citrate sodium, and other reagents were purchased from Sinopharm Chemical Reagent Co., Ltd. (Shanghai, China) and were of analytical grade.

Apparatus

A transmission electron microscope (TEM) (JEOL Ltd., Japan) was used to measure the morphology and internal structure of the DNA hydrogel. The energy-dispersive spectra (EDS) and morphology of the DNA hydrogel were characterized by a scanning electron microscope (SEM) (Carl ZEISS, German). The ultraviolet-visible(UV-vis) absorption spectra were recorded by a UV-1800 spectrophotometer (Shimadzu, Japan).

Preparation of AuNPs

Gold nanoparticles were prepared according to traditional chemical reduction methods, with slight modification. All glassware used in the procedure was thoroughly cleaned in aqua regia (3 parts HCl, 1 part HNO_3) and washed with pure water before use. Briefly, 0.5 mL of 1% $HAuCl_4{\cdot}4H_2O$ was added to 50 mL H_2O and heated until boiling, under vigorous stirring. Then, 0.4 mL of 5% sodium citrate was immediately added to the boiling solution, and the solution was kept boiling for 30 min. The obtained red-wine colloids were cooled to room temperature. The prepared AuNPs were stored at 4 °C in the dark for further use.

SH-PEG was used to ensure the stability of the AuNPs under high salt conditions. 0.25 mL of 5×10^{-5} M SH-PEG was added into 5 mL of prepared AuNPs, and the solution was incubated at 37 °C for 12 h. Then, the supernatant was removed by centrifugation at 10,000 rpm for 10 min, and the

precipitate was dispersed in 30 μL H_2O for further use. The SH-PEG-stabilized AuNPs were characterized by UV-vis and TEM.

Preparation of AuNPs/DNA hydrogel

DNA hydrogel was prepared according to our previous report, with some modifications [28]. Briefly, RCA primer (20 μL, 10^{-5} M) and OTA aptamer (20 μL, 10^{-5} M) were first hybridized by denaturation and purified by exonuclease I (5 μL, 5 U/μL). The purified hybridized product was characterized by 15% native polyacrylamide gel electrophoresis (PAGE). Then, RCA padlock probes (10.5 μL) and T4 ligase (1 μL, 400 U/μL) were added into the hybridized product. After incubation for 30 min, dNTPs (6.4 μL, 10 mM) and Phi29 DNA polymerase (2.0 μL, 10 U/μL) were added to initiate the RCA reaction. After the RCA reaction at 37 °C for 1 h, 5 μL of the above prepared SH-PEG-stabilized AuNPs was added and reacted for another 1.5 h at 37 °C. DNA hydrogel and AuNPs/DNA hydrogel were obtained after standing at 4 °C for 12 h. TEM and SEM were used to characterize the prepared DNA hydrogel.

Photometric detection of OTA using AuNPs/DNA hydrogel

The standard curve of the DNA hydrogel-based detection method was characterized as follows. The purified aptamer-primer hybridized products (10.5 μL) were added to different concentrations of OTA. The solutions were then incubated for 45 min in order to release the free primer for the RCA reaction; the free primer is released due to the competition between OTA and the primer for the aptamer. Then, the AuNPs/DNA hydrogel was prepared according to the method described above. Next, the AuNPs/DNA hydrogel was centrifuged at 2000 rpm for 10 min, and the absorbance of the supernatant at 530 nm was determined using a UV-1800 ultraviolet spectrophotometer. All measurements were repeated three times.

Application in beer samples

Beer samples with three concentrations of OTA added were first refrigerated and then degassed by ultrasound. NaCl (2.57 mol/L) and $NaHCO_3$ (0.24 mol/L) were mixed with buffer. The buffer and beer samples were mixed at a volume ratio of 1:4. The mixtures were then detected using the above method.

Results and discussion

The principle of the aptasensor

A schematic diagram of the colorimetric aptasensor is displayed in Fig. 1. The aptamer and primer were first incubated to form the aptamer-primer hybridized product; the unreacted single-stranded DNA was digested by exonuclease I. In the presence of OTA, the hybridized product was dissociated due to the priority of the combination of the aptamer and OTA compared with that of the aptamer and primer. The dissociation of the hybridized product induced free primer, which is essential for the RCA reaction. The free primer that dissociated from the hybridized product combined with the padlock probe by partially complementary base binding; then, RCA commenced in the presence of T4 DNA ligase and Phi 29 DNA polymerase. The RCA products were obtained, and the DNA hydrogel was subsequently formed by the self-assembly of RCA products. The amount of formed DNA hydrogel was related to the concentration of OTA. With a higher concentration of OTA, more DNA hydrogel was produced. In contrast, the hybridized product could not generate the free primer in the absence of OTA; thus, the DNA hydrogel could not be formed. With the addition of AuNPs into the DNA hydrogel, AuNPs/DNA hydrogel formed. With more DNA hydrogel, there was less AuNPs in the supernatant. Therefore, the concentration of OTA could be monitored by measuring the absorbance of the supernatant.

Characterization of AuNPs

The particle size and dispersibility affect the performance of AuNPs in colorimetric applications. The prepared AuNPs were characterized by UV-vis. A sharp peak appeared at 520 nm, indicating the successful preparation of AuNPs (Fig 2A). SH-PEG-stabilized AuNPs were dispersed in the mixture of T4 ligase buffer and Phi 29 DNA polymerase buffer to ensure their stability in DNA hydrogel. As shown in Fig 2A, there was slight migration of the absorption peak from 520 to 530 nm, which indicates the successful preparation of SH-PEG-modified AuNPs. Further, AuNPs and SH-PEG-modified AuNPs were characterized by TEM. As shown in the TEM image, the prepared AuNPs (Fig. 2B) and SH-PEG-modified AuNPs (Fig. 2C) were both well-dispersed spheres with a diameter of about 14 nm.

Characterization of DNA hydrogel

The successful preparation of aptamer-primer hybridized product is critical for the assay. Thus, 15% native PAGE was used to verify this. As shown in Fig. S1, the locations of the aptamer-primer hybridized product (lane 4), aptamer (lane 2), and primer (lane 3) showed that the hybridized

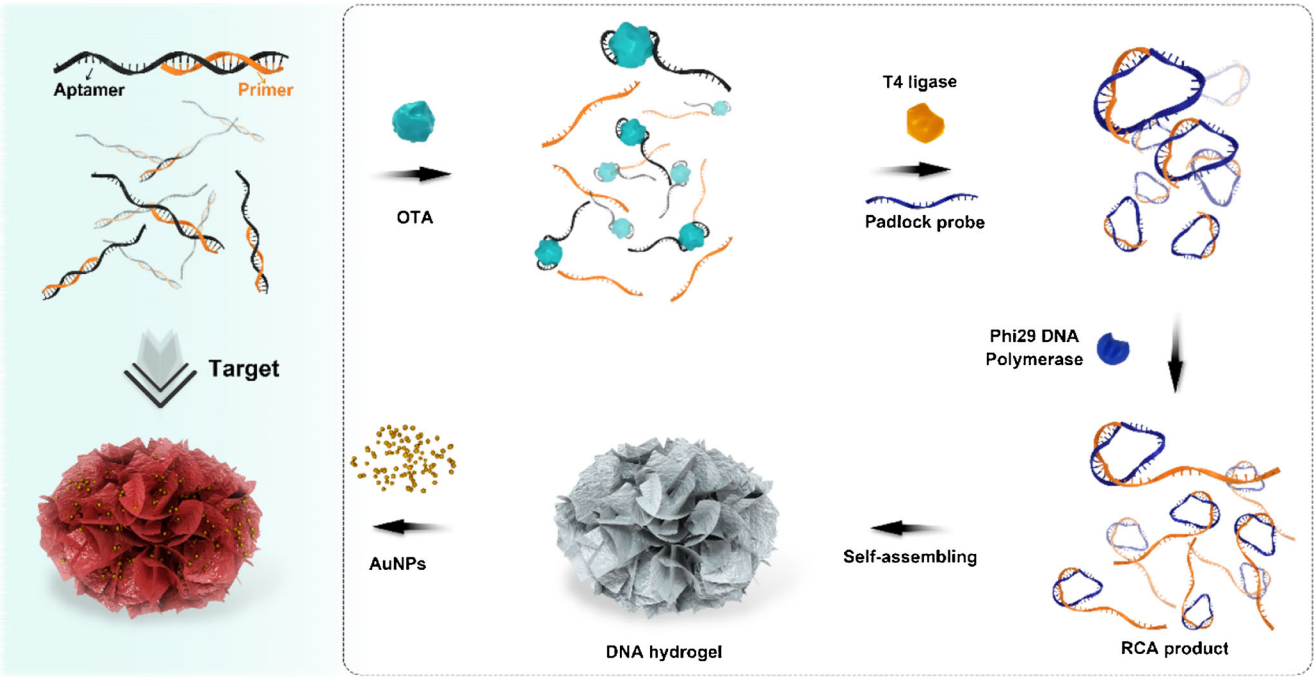

Fig. 1 Diagram of the principle of the colorimetric aptasensor for OTA detection based on rolling circle amplification product self-assembled DNA hydrogel

product had a slower migration velocity than the aptamer and primer. The main reason for the slower migration velocity of lane 4 is the increase in the base number, indicating that the hybridized product was successfully prepared. The aptamer-primer hybridized product was further purified for the digesting of single-stranded DNA by exonuclease I. No other bands in lane 5 were observed, indicating that the hybridized product was pure.

In the presence of OTA, the aptamer-primer complex partially melts due to the competition for combination with the aptamer between the OTA and primer. As a result, free primer is released, and RCA commences after the addition of T4 ligase, Phi29 DNA polymerase, and dNTPs. The RCA product was characterized by native PAGE (Fig. S1 Lane 6). The bright band in the loading well in lane 6 indicates that there was a large number of bases in the RCA product, so the RCA product could not migrate from the loading well. This indicates that the RCA reaction was successfully started.

The TEM and SEM images in Fig. 3A show that the DNA hydrogel prepared in this work was viscous with a three-

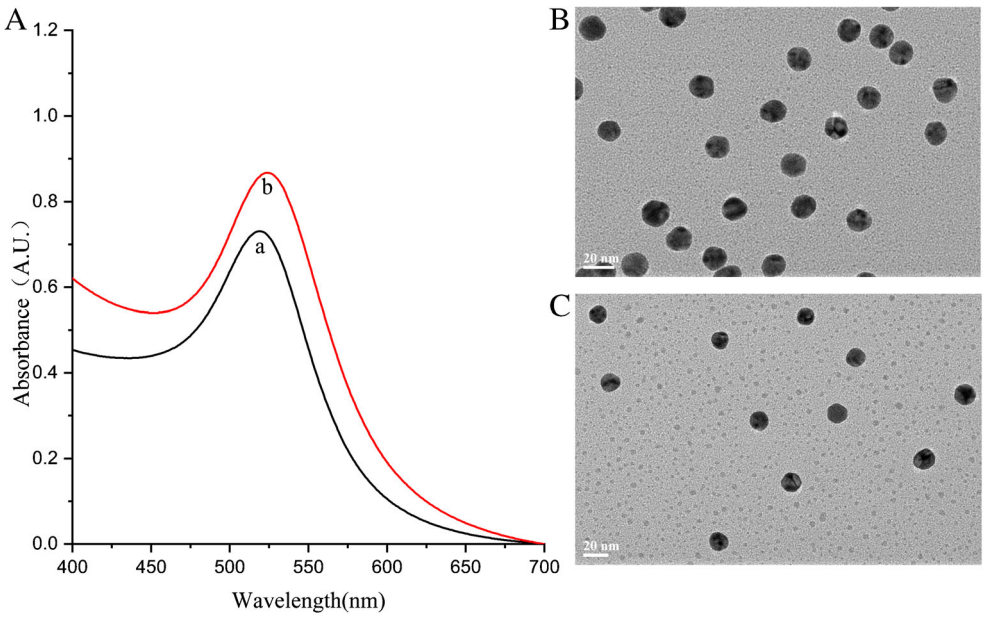

Fig. 2 A UV-vis spectra of AuNPs (a) and SH-PEG-modified AuNPs (b); B TEM image of AuNPs; C TEM image of SH-PEG-modified AuNPs

dimensional micrometre-sized flower-like shape. Furthermore, the distribution of the elements was characterized by EDS elemental mapping. The results in Fig. 3B and Fig. 3C indicate that the element composition included C, P, N, O, P, and Mg. Further, the element distribution of the DNA hydrogel was obtained by merging the distributions of C, N, and Mg, respectively. The results in Fig. 3C indicate that the distribution of Mg was more central in the DNA hydrogel than at the boundary. Therefore, the possible formation mechanism may first involve the formation of Mg_2PPi crystals and then the combination of DNA with the Mg_2PPi crystals to form complexes, resulting in the formation of the DNA hydrogel.

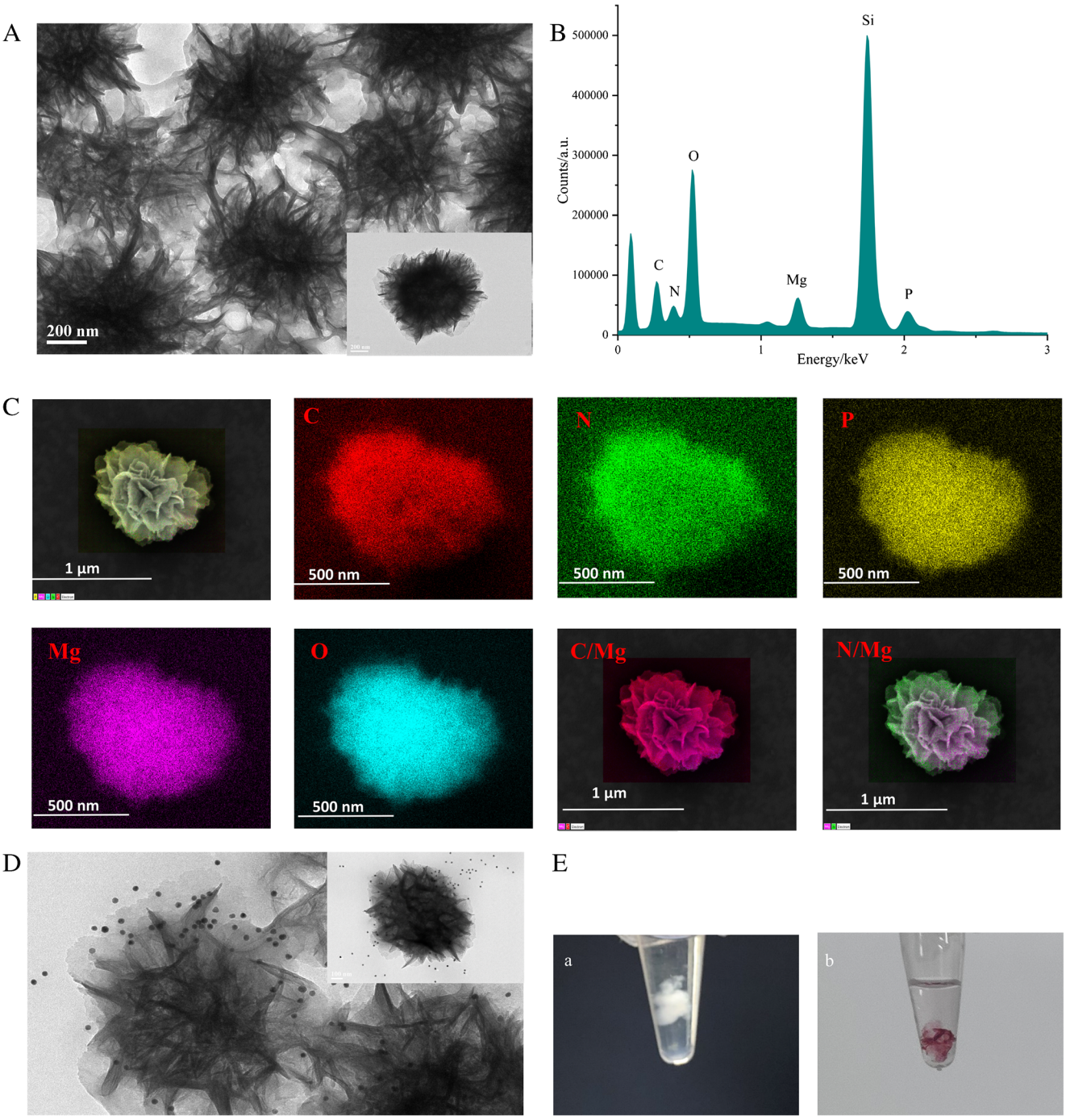

Fig. 3 A Morphology characterization of the prepared DNA hydrogel by TEM; B energy-dispersive spectroscopy (EDS) spectra of the DNA hydrogel; C morphology and elemental characterization of the prepared DNA hydrogel by SEM; D TEM image of AuNPs/DNA hydrogel; E photos of the DNA hydrogel (a) and AuNPs/DNA hydrogel (b)

Poly T bases were added into the padlock probe sequences to obtain poly A bases in the RCA product and DNA hydrogel. The DNA hydrogel with the padlock probe containing poly T bases can easily bind with AuNPs due to the strong binding force between poly A bases and AuNPs, resulting in the formation of AuNPs/DNA hydrogel. The morphology of the AuNPs/DNA hydrogel was also characterized by TEM. As shown in Fig. 3D, the morphology of the AuNPs/DNA hydrogel was similar to the DNA hydrogel, with a viscous three-dimensional micrometre-sized flower-like shape. The AuNPs were enclosed by the DNA hydrogel to form AuNPs/DNA hydrogel. Photos of the DNA hydrogel and AuNPs/DNA hydrogel were also taken and are shown in Fig. 3E. The DNA hydrogel turned red and could be observed by the naked eye, also indicating that the AuNPs were enclosed, and the AuNPs/DNA hydrogel was formed. Together, these results demonstrate that AuNPs can be immobilized inside DNA hydrogel by modifying the padlock probe DNA sequences with more T bases, avoiding the need to modify AuNPs with DNA sequences.

Optimization of experimental conditions

The amount of AuNPs added to the DNA hydrogel was optimized. DNA hydrogel was prepared as described above. The amounts of AuNPs tested were as follows: 0 μL, 2.5 μL, 5 μL, 7.5 μL, and 10 μL. The DNA hydrogel and AuNP mixture stood at 4 °C for 12 h to form the AuNPs/DNA hydrogel.

Then, the supernatant was obtained by centrifugation of the hydrogel at 2000 rpm for 10 min, and the absorbance of the supernatant was determined. As shown in Fig. 4A, when the amount of AuNPs was less than 5 μL, the absorbance of the supernatant at 530 nm was almost zero, and when the amount of AuNPs was more than 5 μL, the absorbance of the supernatant at 530 nm began to increase. The possible reason for this is that the hydrogel was saturated by AuNPs with the 5 μL amount of AuNPs. Therefore, 5 μL AuNPs was selected as optimal.

The morphology of the DNA hydrogel may affect the combination of AuNPs with the DNA hydrogel. Thus, the effect of reaction time on the morphology of the DNA hydrogel was investigated. The morphology of the DNA hydrogel at different reaction times (0.5 h, 1.0 h, 1.5 h, 2.0 h, 2.5 h, and 3.0 h) was recorded by SEM with an OTA concentration of 10 ng/mL. As shown in Fig. 4B, the size of the DNA hydrogel first increased and then remained constant with the tightening of the internal formation.

Then, the effects of reaction time (1 h, 1.5 h, 2.0 h, 2.5 h, and 3.0 h) on the absorbance of the supernatant with 10 ng/mL OTA and 5 μL AuNPs were studied. The results are shown in Fig. 4C. With an increase in reaction time, the UV-vis absorbance of the supernatant at 530 nm first decreased and then reached a plateau, which may be because the DNA hydrogel was saturated by AuNPs after 2.5 h. The morphology of the DNA hydrogel remained stable at the reaction time of 2.5 h. Therefore, the optimal total reaction time for the DNA hydrogel and AuNPs/DNA hydrogel was determined to be 2.5 h.

Analytical performance

In the presence of OTA, melting of the aptamer-primer hybridized product occurred, and the DNA hydrogel was generated. The amount of DNA hydrogel was related to the concentration of OTA. When AuNPs were added into the DNA hydrogel, some of the AuNPs were enclosed inside the DNA hydrogel; the more the DNA hydrogel, the more AuNPs that were enclosed. Thus, the absorbance of AuNPs in the supernatant was negatively related to the concentration of OTA.

As shown in Fig. 5A and 5B, with an increasing concentration of OTA, the absorbance of the supernatant at 530 nm decreased. Under optimal conditions, the ΔOD (ΔOD = OD_0-OD; OD_0 and OD represent the background absorbance and the absorbance in the presence of OTA, respectively) was negatively correlated with the logarithm of the concentration of OTA. In the OTA concentration range of 0.05 to 10 ng/mL, the ΔOD and OTA concentration were linearly correlated, with the equation of $Y = 5722–0.1911*X$ ($R = 0.9941$). The detection limit of OTA was calculated to be 0.005 ng/mL using the equation $LOD = 3SD/m$, where SD is the standard deviation of the blank and m is the slope of the calibration plot.

Colorimetric detection is considered to be one of the most promising and efficient methods for on-site detection; however, the detection limit is important for this detection method. The detection limit of the developed method in this work is lower than that of most of the published colorimetric detection methods (Table S2); this is mainly due to the DNA hydrogel detection strategy used in this work. In most previous methods that use the target-induced collapse of DNA hydrogel detection mode, the sensitivity is poor because the collapse of the DNA hydrogel requires a large amount of target. In this work, the DNA hydrogel was formed by self-assembly of the RCA products in the presence of OTA. Due to the signal amplification of RCA and the self-assembly of RCA products, a small amount of OTA causes the formation of DNA hydrogel. Thus, the sensitivity of the detection method is greatly improved.

In addition, samples of 10 ng/mL OTA were determined to have a relative standard deviation (RSD) of 3.57% (10 ng/mL, $n = 6$), which means that the stability and precision of the aptasensor meet the detection requirements.

Specificity is one of the most important properties of biosensors. The specificity of the developed DNA hydrogel aptasensor for OTA was assessed. Several other mycotoxins were selected and tested under the same experimental conditions as those used for OTA. The relative absorbance ratio (ΔOD) was obtained by the formula $(OD_0\text{-}OD)/(OD_0\text{-}OD_A)$, where OD_0 represents the supernatant absorbance of the blank sample, OD represents the supernatant absorbance of the other

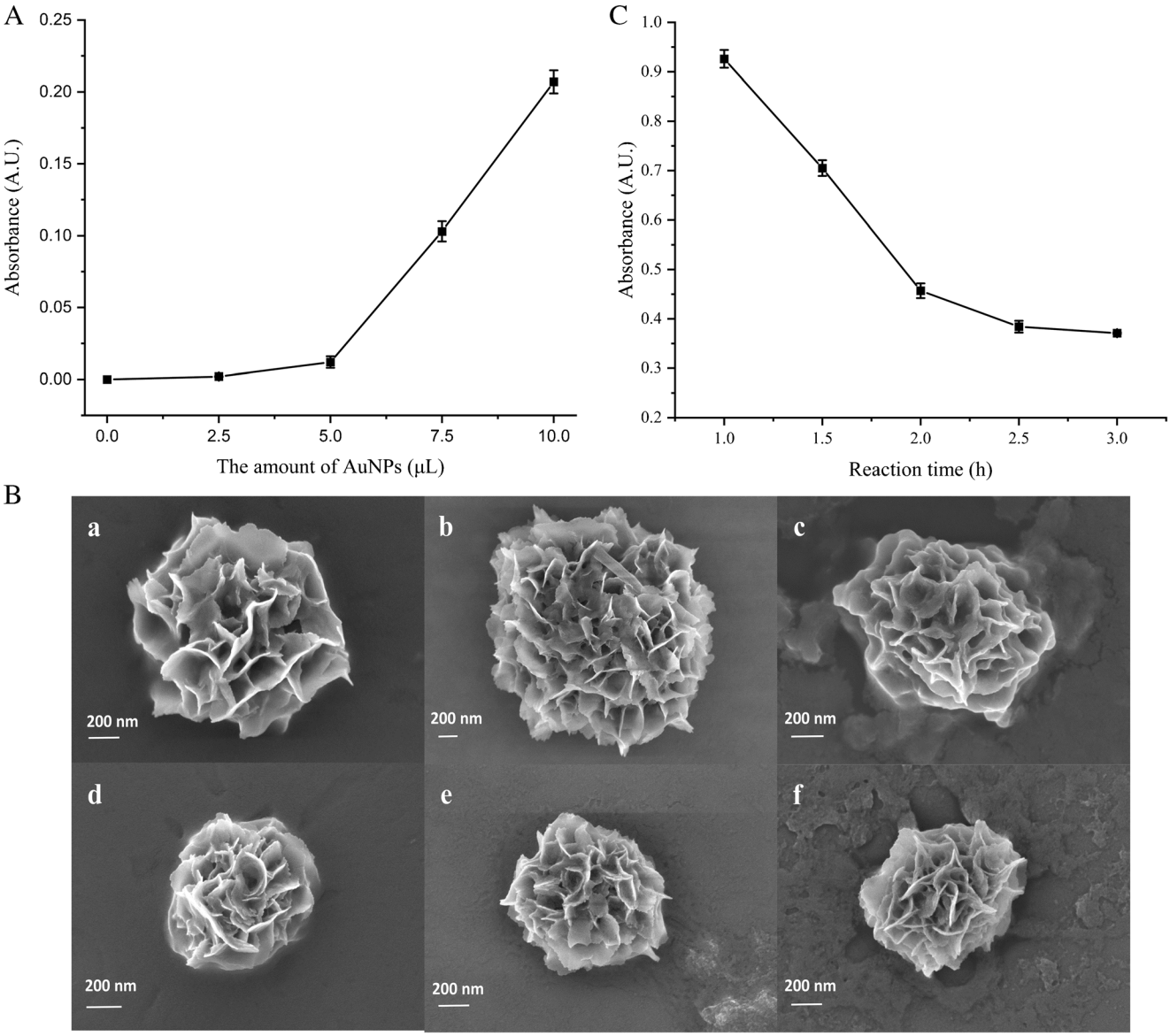

Fig. 4 A The effect of the amount of AuNPs added (0 μL, 2.5 μL, 5 μL, 7.5 μL, 10 μL) on the absorbance of the supernatant at 530 nm; B SEM images of the DNA hydrogel at different reaction times: a 0.5 h, b 1.0 h, c 1.5 h, d 2.0 h, e 2.5 h, f 3.0 h; C the effect of different reaction times (1.0 h, 1.5 h, 2.0 h, 2.5 h, and 3.0 h) on the absorbance of the supernatant at 530 nm

four toxins, and OD_A represents the supernatant absorbance of OTA. As shown in Fig. 5C, the absorbance changes caused by other mycotoxins were much smaller than that caused by OTA, which indicates that the fabricated DNA hydrogel aptasensor possesses good specificity for OTA. This is mainly due to the good specificity of the OTA aptamer and the reasonable design of the sequences of the primer and padlock probe.

In addition, the developed aptasensor was applied to real samples. The European Union and the Chinese government have set the maximum limits of OTA in barley and malt, which are the main raw materials for beer production and are considered the main pollution sources for OTA in beer. Artificially contaminated beer was used as a real sample model. The concentrations used in this test were 1 ng/mL, 2 ng/mL, and 10 ng/mL. The commercial ELISA method and the proposed method detection results are summarized in Table 1. The results obtained by the two methods were similar. The recoveries ranged from 92.8 to 103.5%, which corresponds with the results obtained from ELISA, indicating that the accuracy of the developed method is good.

Conclusion

In conclusion, we have developed a versatile colorimetric method to improve the sensitivity of DNA hydrogel-based OTA

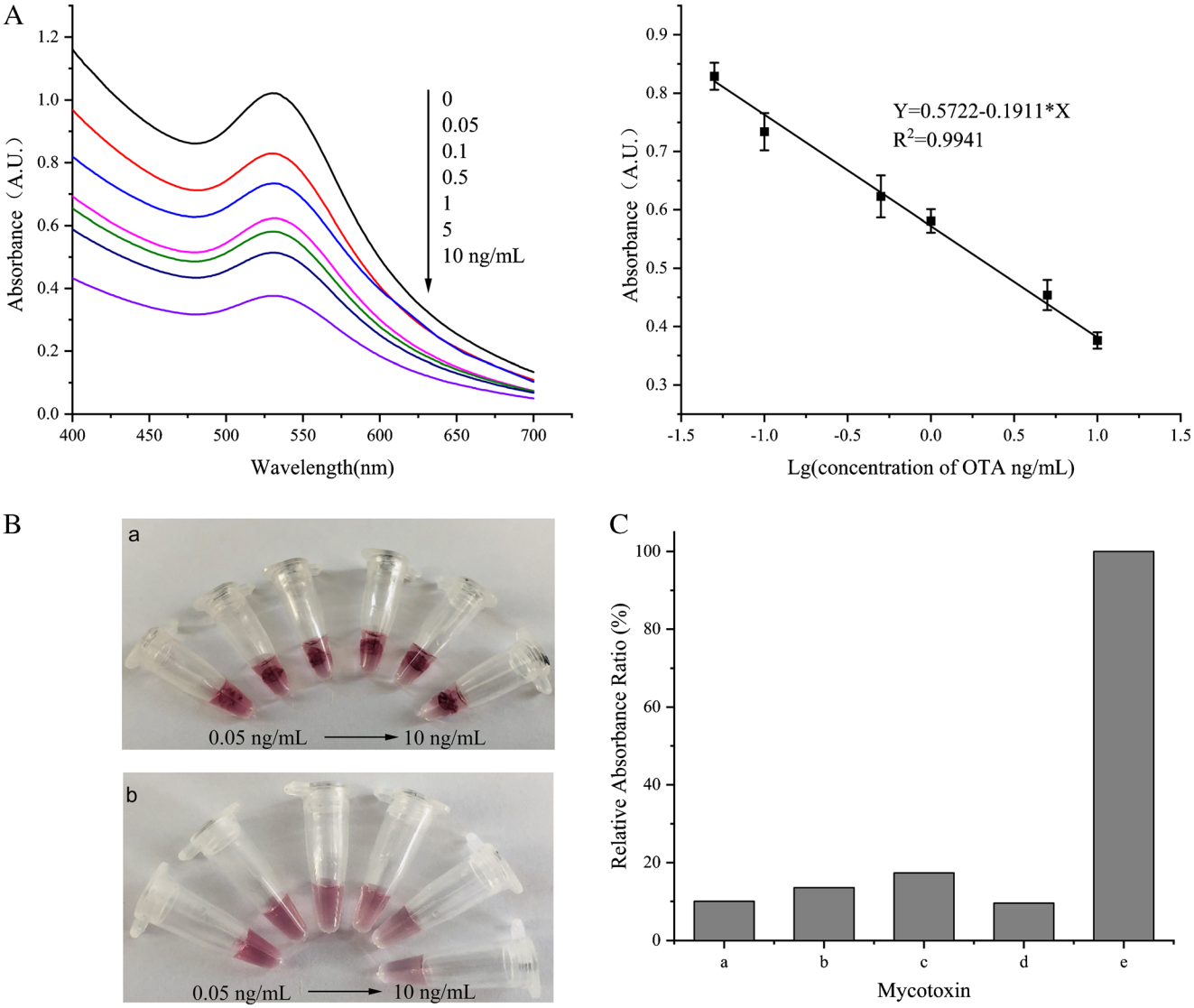

Fig. 5 A The absorbance spectra of the supernatant at different concentrations of OTA and the linear relationship between the absorbance of the supernatant at 530 nm and the logarithm of OTA concentration measured by the aptasensor; B photos of the AuNPs/DNA hydrogel (a) and supernatant (b) with a series of concentrations of OTA; C specificity verification of the detection method for OTA with other mycotoxins: a OTB, b AFB1, c ZEN, d T-2, and e OTA

Table 1 Results of recovery rates of standard addition and RSD of the developed aptasensor

Items	Added concentration (ng/mL)	Results determined by ELISA (ng/mL)	Recovery rate calculated by ELISA	Results obtained by this method (ng/mL)	Recovery calculated by this method	RSD of this method
Beer	1	0.965±0.05	96.5%	0.928±0.05	92.8%	5.39%
Beer	1	0.972±0.04	97.2%	0.949±0.05	94.9%	5.27%
Beer	2	2.10±0.07	105.0%	2.07±0.11	103.5%	5.31%
Beer	2	1.96±0.10	98.0%	2.05±0.09	102.5%	4.39%
Beer	10	9.51±0.35	95.1%	9.82±0.32	98.2%	3.26%
Beer	10	9.38±0.33	93.8%	9.57±0.37	95.7%	3.87%

detection. Unlike the previously reported DNA hydrogel-based detection modes, the formation of the DNA hydrogel was induced by the target. In this mode, the target combines with the aptamer, resulting in the release of the partially complementary sequence which, in turn, initiates RCA, resulting in the formation of DNA hydrogel. The combination of the aptamer with the RCA product-based DNA hydrogel makes the both mutually supportive to improve the detection limit of visual detection. Meanwhile, AuNPs without DNA sequence modification can be directly assembled inside the DNA hydrogel by adjusting the padlock probe sequences with the addition of poly T bases, due to the stronger binding force between poly A bases and AuNPs. As a result, under optimal experimental conditions, highly sensitive performance of the DNA hydrogel-based visual detection method, with a detection limit of 5 pg/mL for OTA, was observed. Further, the accuracy of the developed detection method was evaluated by comparing it with a commercial ELISA kit, and the results showed good accuracy. The aptasensor was also successfully applied to actual beer samples. Due to the high stability and good specificity of the aptamer, the developed aptasensor has potential applications in other foods, after selection of the optimal pretreatment method. However, the costs of T4 DNA ligase and Phi 29 DNA polymerase, which are necessary for the RCA process, are a little high, which may limit the application of this DNA hydrogel for fast detection. It remains a challenge and a goal to further reduce the cost of the detection method, such as by seeking lower cost enzymes and so on in the future.

Supplementary Information The online version contains supplementary material available at https://doi.org/10.1007/s00604-021-05000-y.

Funding This work was partly supported by the Science and Technology Innovation Action Plan of Shanghai (20392001600), the Natural Science Foundation of Shanghai (18ZR1409500), and the Technology R&D Program of Suzhou (SNG2018044).

Declarations

Conflict of interest The authors declare that they have no conflict of interest.

References

1. Tao YF, Xie SY, Xu FF, Liu AM, Wang YX, Chen DM, Pan YH, Huang LL, Peng DP, Wang X, Yuan ZH (2018) Ochratoxin A: toxicity, oxidative stress and metabolism. Food Chem Toxicol 112:320–331
2. el Khoury A, Atoui A (2010) Ochratoxin A: general overview and actual molecular status. Toxins 2(4):461–493
3. Pfohl-Leszkowicz A, Manderville RA (2007) Ochratoxin A: an overview on toxicity and carcinogenicity in animals and humans. Mol Nutr Food Res 51(1):61–99
4. (2006) European Commission Regulation Setting maximum levels for certain contaminants in foodstuffs. No. 1881/2006 of 19 December 2006 Off J Eur Union 364:5–24
5. Suea-Ngam A, Deck L-T, Howes PD, deMello AJ (2020) An ultrasensitive non-noble metal colorimetric assay using starch-iodide complexation for ochratoxin A detection. Anal Chim Acta 1135: 29–37
6. Zhu H, Liu C, Liu X, Quan Z, Liu W, Liu Y (2021) A multicolorimetric immunosensor for visual detection of ochratoxin A by mimetic enzyme etching of gold nanobipyramids. Microchim Acta 188(3):62
7. Liu M, Li X, Li B, Du J, Yang Z (2020) A fluorometric aptamer-based assay for ochratoxin A by using exonuclease III-assisted recycling amplification. Microchim Acta 187(1)
8. He Y, Tian F, Zhou J, Jiao B (2019) A fluorescent aptasensor for ochratoxin A detection based on enzymatically generated copper nanoparticles with a polythymine scaffold. Microchim Acta 186(3): 199
9. Savastano ML, Losito I, Pati S (2016) Rapid and automatable determination of ochratoxin A in wine based on microextraction by packed sorbent followed by HPLC-FLD. Food Control 68:391–398
10. Ding Y, Shang H, Wang X, Chen L (2020) A SERS-based competitive immunoassay for highly sensitive and specific detection of ochratoxin A. Analyst 145(18):6079–6084
11. Nagahara S, Matsuda T (1996) Hydrogel formation via hybridization of oligonucleotides derivatized in water-soluble vinyl polymers. Polymer Gels Netw 4(2):111–127
12. Kouwer PHJ, Koepf M, Le Sage VAA, Jaspers M, van Buul AM, Eksteen-Akeroyd ZH, Woltinge T, Schwartz E, Kitto HJ, Hoogenboom R, Picken SJ, Nolte RJM, Mendes E, Rowan AE (2013) Responsive biomimetic networks from polyisocyanopeptide hydrogels. Nature 493:651–655
13. Li J, Mo L, Lu C-H, Fu T, Yang H-H, Tan W (2016) Functional nucleic acid-based hydrogels for bioanalytical and biomedical applications. Chem Soc Rev 45(5):1410–1431
14. Song JY, He WT, Shen H, Zhou ZX, Li MQ, Su P, Yang Y (2019)Self-assembly of a magnetic DNA hydrogel as a new biomaterial for enzyme encapsulation with enhanced activity and stability. Chem Commun 55(17):2449–2452
15. Mao Y, Li JX, Yan JM, Ma YL, Song YL, Tian T, Liu X, Zhu Z, Zhou LJ, Yang CY (2017) A portable visual detection method based on a target-responsive DNA hydrogel and color change of gold nanorods. Chem Commun 53(47):6375–6378
16. Liao WC, Lilienthal S, Kahn JS, Riutin M, Sohn YS, Nechushtai R, Willner I (2017)pH- and ligand-induced release of loads from DNA-acrylamide hydrogel microcapsules. Chem Sci 8(5):3362–3373
17. Chang YY, Li MY, Wu ZY, Zhuo Y, Chai YQ, Xiao Q, Yuan R (2018) Homogeneous entropy catalytic-driven DNA hydrogel as strong signal blocker for highly sensitive electrochemical detection of platelet-derived growth factor. Anal Chem 90(13):8241–8247
18. Liu RD, Huang YS, Ma YL, Jia SS, Gao MX, Li JX, Zhang HM, Xu DM, Wu M, Chen Y, Zhu Z, Yang CY (2015) Design and synthesis of target-responsiveaptamer-cross-linked hydrogel for visual quantitative detection of ochratoxin A. ACS Appl Mater Interfaces 7(12):6982–6990
19. Si Y, Li L, Wang N, Zheng J, Yang R, Li J (2019) Oligonucleotide cross-linked hydrogel for recognition and quantitation of MicroRNAs based on a portable glucometer readout. ACS Appl Mater Interfaces 11(8):7792–7799
20. Li YS, Ma YL, Jiao XY, Li TY, Lv ZH, Yang CJ, Zhang XJ, Wen YQ (2019) Control of capillary behavior through target-responsive hydrogel permeability alteration for sensitive visual quantitative detection. Nat Commun 10:1036

21. Geng JH, Yao C, Kou XH, Tang JP, Luo D, Yang DY (2018) A fluorescent biofunctional DNA hydrogel prepared by enzymatic polymerization. Adv Healthcare Mater 7(5):1700998
22. Huang YS, Xu WL, Liu GY, Tian LL (2017) A pure DNA hydrogel with stable catalytic ability produced by one-step rolling circle amplification. Chem Commun 53(21):3038–3041
23. Yan YC, Li J, Li WH, Wang Y, Song WL, Bi S (2018) DNA flower-encapsulated horseradish peroxidase with enhanced biocatalytic activity synthesized by an isothermal one-pot method based on rolling circle amplification. Nanoscale 10(47):22456–22465
24. Xie SB, Zhang J, Teng LM, Yuan W, Tang Y, Peng Q, Tang QC (2019) Electrochemical detection of lipopolysaccharide based on rolling circle amplification assisted formation of copper nanoparticles for enhanced resistance generation. Sensors Actuators B-Chem 301:127072
25. Li X, Cui Y, Du Y, Tang A, Kong D (2019)Label-free telomerase detection in single cell using a five-base telomerase product-triggered exponential rolling circle amplification strategy. ACS Sensors 4(4):1090–1096
26. Liu X, Song M, Hou T, Li F (2017)Label-free homogeneous electroanalytical platform for pesticide detection based on acetylcholinesterase-mediated DNA conformational switch integrated with rolling circle amplification. ACS Sensors 2(4):562–568
27. Liu M, Zhang Q, Kannan B, Botton GA, Yang J, Soleymani L, Brennan JD, Li Y (2018)Self-assembled functional DNA superstructures as high-density and versatile recognition elements for printed paper sensors. Angewandte Chem-Int Edition 57(38): 12440–12443
28. Hao L, Wang W, Shen X, Wang S, Li Q, An F, Wu S (2020) A fluorescent DNA hydrogel aptasensor based on the self-assembly of rolling circle amplification products for sensitive detection of ochratoxin A. J Agric Food Chem 68(1):369–375